

This article was downloaded by: [Renmin University of China]

On: 13 October 2013, At: 11:34

Publisher: Taylor & Francis

Informa Ltd Registered in England and Wales Registered Number: 1072954 Registered office: Mortimer House, 37-41 Mortimer Street, London W1T 3JH, UK



## Advanced Composite Materials

Publication details, including instructions for authors and subscription information:

<http://www.tandfonline.com/loi/tacm20>

### Analysis and finite element simulation of the draping process of multilayer knit structures and the effects of a localized fixation

O. Döbrich<sup>a</sup>, T. Gereke<sup>a</sup>, C. Cherif<sup>a</sup> & S. Krzywinski<sup>a</sup>

<sup>a</sup> Institute of Textile Machinery and High Performance Material Technology, Faculty of Mechanical Science and Engineering, Technische Universität Dresden, Hohe Straße 6, Dresden, 01062, Germany

Published online: 03 May 2013.

To cite this article: O. Döbrich, T. Gereke, C. Cherif & S. Krzywinski (2013) Analysis and finite element simulation of the draping process of multilayer knit structures and the effects of a localized fixation, *Advanced Composite Materials*, 22:3, 175-189, DOI: [10.1080/09243046.2013.791239](https://doi.org/10.1080/09243046.2013.791239)

To link to this article: <http://dx.doi.org/10.1080/09243046.2013.791239>

PLEASE SCROLL DOWN FOR ARTICLE

Taylor & Francis makes every effort to ensure the accuracy of all the information (the "Content") contained in the publications on our platform. However, Taylor & Francis, our agents, and our licensors make no representations or warranties whatsoever as to the accuracy, completeness, or suitability for any purpose of the Content. Any opinions and views expressed in this publication are the opinions and views of the authors, and are not the views of or endorsed by Taylor & Francis. The accuracy of the Content should not be relied upon and should be independently verified with primary sources of information. Taylor and Francis shall not be liable for any losses, actions, claims, proceedings, demands, costs, expenses, damages, and other liabilities whatsoever or howsoever caused arising directly or indirectly in connection with, in relation to or arising out of the use of the Content.

This article may be used for research, teaching, and private study purposes. Any substantial or systematic reproduction, redistribution, reselling, loan, sub-licensing, systematic supply, or distribution in any form to anyone is expressly forbidden. Terms &



## Analysis and finite element simulation of the draping process of multilayer knit structures and the effects of a localized fixation

O. Döbrich\*, T. Gereke, C. Cherif and S. Krzywinski

*Institute of Textile Machinery and High Performance Material Technology, Faculty of Mechanical Science and Engineering, Technische Universität Dresden, Hohe Straße 6, Dresden 01062, Germany*

*(Received 29 February 2012; accepted 27 March 2013)*

Fiber reinforced composites (FRC) are an interesting alternative for numerous applications due to their lightweight character. However, there are currently several challenges for a serial production. The manufacturing process still requires a high percentage of manual labor which greatly restricts the reproducibility. Additionally, high-quality standards necessary for many applications cannot be met due to the low displacement resistance of the textiles. Structural fixation could greatly improve the displacement resistance and therefore the handling of the material layers. This paper reports on a model used for draping simulations of nonfixed and fixed multilayer knits using the commercial finite element software LS-DYNA<sup>®</sup>. The aim of this model is to improve the development process of FRCs. With a standardized specification, the basic macromechanical properties can be modeled with finite shell elements. A material model is introduced that accounts to the characteristic mechanisms of the deformation of biaxial fibrous structures. A fixation of the fabrics is achieved by melting the thermoplastic hybrid yarns embedded in the textile structure with infrared radiation. This process improves the handling of the textiles. It is of great benefit when such a structural fixation is applied locally. The process of choosing local fixation zones is described in this paper and the applicability of this process is illustrated.

**Keywords:** fabrics/textiles; preform; finite element analysis (FEA); forming; drape simulation

### 1. Introduction

The need for innovative lightweight engineering solutions is greater than ever before. Economic and ecological imperatives drive the search forward for new high-performance materials. Increasingly, composite materials are gaining attention in the fields of engineering. With these materials, a higher efficiency in mass-specific material to component stiffness can be achieved. The anisotropic characteristics of fiber reinforced composites (FRC) allow the designer to optimize their load-bearing capacities. Components made of FRC can be molded into complex forms designed to carry heavy loads. The ability to mass produce such FRC components would pre-destine their increased application in the automotive and mechanical engineering industries. To date, the manufacturing chain of continuous FRC includes the step of preforming. In this intermediate step, quality standards, as required in high-technology fields cannot be met at present. Due to inadequate stiffness and consequent shifting of the yarns in their placement to one another, the handling of the preforms during the pre-cutting

---

\*Corresponding author. Email: [oliver.doebrich@tu-dresden.de](mailto:oliver.doebrich@tu-dresden.de)

process or shipment can cause massive changes in the geometry of the fiber layers. The placement of the fiber layers plays a key role in the end performance of the component as the mechanical potential of the continuous fiber reinforcement depends on the crimping of the yarns and the force-oriented arrangement of the individual fiber layers. Specifically, for components that are formed three-dimensionally, it is necessary to know where the fibers are located after the draping process to ensure a correct force-oriented design.

The application of thermoplastic-based multilayer knits as a basis for FRCs has proven to be advantageous.[1] To lend the group of continuous reinforced composites a competitive edge, computer simulations can be used in the development phase. The focus lies on improving the preform handling by performing a prefixation of the fabric. Hybrid yarns can be incorporated during the construction of the textile structure without additional steps or effort. The thermoplastic threads can be incorporated either in a grid pattern or over the entire area depending on the type of preform desired and can be melted directly after the knitting process. Through the localized fixation, a positive effect on the stiffness and the stability of the yarn is achieved and in turn, the handling properties and the drapability of the textile are improved.

In selecting the areas for local fixation, later-shaping processes must be considered. For this purpose, local fixation models created with the knowledge of the final textile's drapability characteristics are necessary before the actual production of the textile begins. Determining the fixation zones with an experimentally-based trial-and-error method would involve exorbitantly high production costs, efforts, and long development times. To solve this problem, the aim is a simulation-supported development of hybrid yarn-based preforms that can be pre-consolidated for structure fixation. Therefore, this paper deals with special problems in drape simulation. Many efforts were made in this field of research in the last decades. A comprehensive summarization on this topic was made by Gereke et al. [2].

## 2. Structure fixation by incorporating hybrid yarns

Hybrid yarns are mixed yarns made of different types of material. In this study, an air-texturized glass/polypropylene (GF/PP) yarn was used. The incorporation of the hybrid yarns in the multilayer knit occurs directly during the production process in the form of reinforcement and/or knitting threads. The fusion of the thermoplastic yarns is accomplished using infrared radiation. The fusion stiffens the thermoplastic part of the multifilament yarns and bonds the reinforcing thread with the adjoining threads at the points of intersection. The effects deemed from this type of fixation can be seen in Figure 1. A significant increase in the rigidity of the

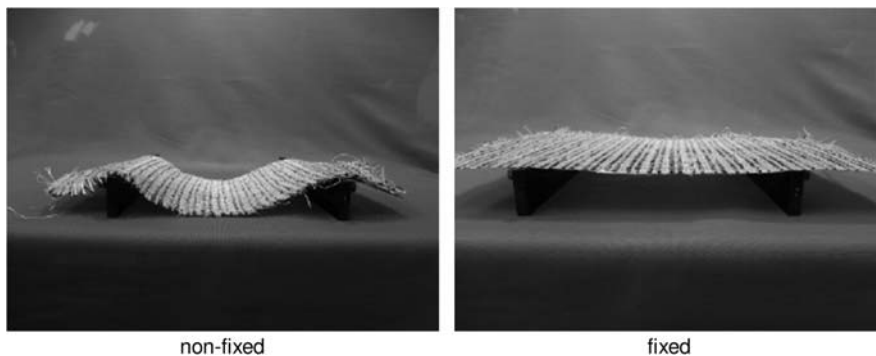

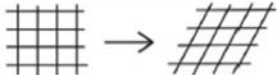
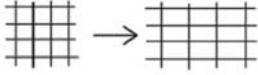

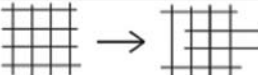
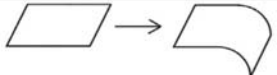


Figure 1. Increase in textile rigidity by a holohedral fixation of the textile structure.

Table 1. Deformation mechanisms in textile semi-finished goods according to [3,4].

Mechanism	Scheme	Mechanism	Scheme
Extension		Shear	
Elongation		Sliding	
Slippage		Bending	

fixed textile can be observed with just a small ratio of fixation threads (Figure 1 shows sample M1.7 according to Table 2). This leads to better handling and offers many advantages in the transportation and relocation of the preform. Furthermore, this effect can be used to achieve the desired drapability properties.

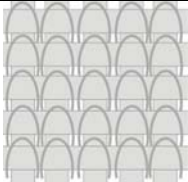


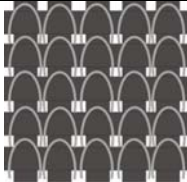





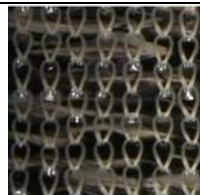
### 3. Deformation mechanisms in textile materials

The following mechanisms in the draping behavior define the types of in-plane deformation occurring in textile materials. They will be used to characterize the macroscopic deformation behavior. The individual deformation modes are the basis for the requirements on the material model. They aid in understanding and describing the complex in-plane deformations. The mechanisms can be evaluated for their relevance according to the design of the textile. In Table 1, the most important deformation mechanisms for the draping simulation are listed according to references [3,4]. The character of the individual mechanisms can be defined using engineering constants. The constants can be determined using standardized textile tests. Extension and elongation are examined as an entity and registered as the tensile rigidity observed in the main reinforcing directions. Due to the shear strain, especially with less rigid textiles, the potential for deformation is very high. The resistance against shearing can be specified with a modulus of rigidity. Sliding and slippage are in-plane deformation mechanisms and are largely dependent on the microscopic composition of the fabric. Multilayer knits with a loose-knitting thread system are prone to increased deformation due to slippage. Sliding is somewhat restricted by the knitting threads. The resistance to sliding depends on the knitting thread tension. Bending is the only out-of-plane deformation mechanism.

### 4. Mechanical analysis of the textile structures

Various samples of biaxial knit fabrics were analyzed to investigate the mechanical properties of fixed and nonfixed multilayer knits. Table 2 lists the parameters of the individual textile semi-finished products. The amount of reinforcing GFs is identical in all the samples. The sample VS is a multilayer knit composed of pure glass yarns and is included as a reference

Table 2. Parameters of the multi-layer knit samples (EC–electric glass fiber, GF–glass fiber, PP–polypropylene).

Sample	Biaxial knit ‘VS’	Biaxial knit ‘VS2’	Biaxial knit ‘M1.7’	Biaxial knit ‘M4’
Warp system	EC-GF 900tex	EC-GF+PP 1200tex	Yarns 2, 4 out of 5: EC-GF 900tex Yarns 1, 3, 5 out of 5: EC-GF+PP 1200tex	EC-GF+PP 1200tex
Weft system	EC-GF 900tex	EC-GF+PP 1200tex	Yarns 2, 4 out of 5: EC-GF 900tex Yarns 1, 3, 5 out of 5: EC-GF+PP 1200tex	EC-GF+PP 1200tex
Knitting threads	EC-GF 3 x 34tex	EC-GF+PP 137tex	EC-GF 3 x 34tex	EC-GF 3 x 34tex
Scheme of the sample				
	Glas fiber:  Hybrid yarn:  (900tex GF + 300tex PP)			
Picture of the sample				

sample. This sample cannot be fixed. To evaluate the deformation mechanisms listed, standard testing methods were used. The strip tensile method (DIN EN ISO 13934-1) was used to test the elongation and extension in the direction of the alignment of the main reinforcement threads. Figure 2 presents the results of the strip tensile tests for nonfixed and fixed samples in the 0° direction up to 1% strain. It was observed that the tensile modulus decreased as the amount of hybrid yarn in the structure increased.

Swirls form during the yarn commingling process. Applied axial tensile forces compensate those swirls. This leads to a rather low-tensile modulus in the beginning of the loading. The effects of tensile rigidity are negligible in technical textiles comprised of high-performance fibers, such as glass or carbon. As shown in Figure 2, the rigidity of sample VS2 does not change significantly after the thermofixation. This is due to the small amount of hybrid yarns in the VS2 fabric which were inserted as knit yarns only. There is no amount of hybrid yarns in the main reinforcement directions. An interesting effect can be spotted when comparing the samples M1.7 and M4. The influence of the fixation on the tensile modulus is the most significant in samples M4. This is due to the thermofixed hybrid yarns in the warp and weft directions. The hybrid yarns are consolidated and an elastic material behavior of the PP and glass hybrid yarns replaces the strain due to swirl compensation in the nonfixed samples. In the fixed M1.7 samples, the hybrid yarns are consolidated and they are bounded to the glass yarns where they cross each other. Thus, each reinforcing glass yarn is in some points fixated by the thermoplastic matrix. Local stress peaks at those crossing points of glass yarns

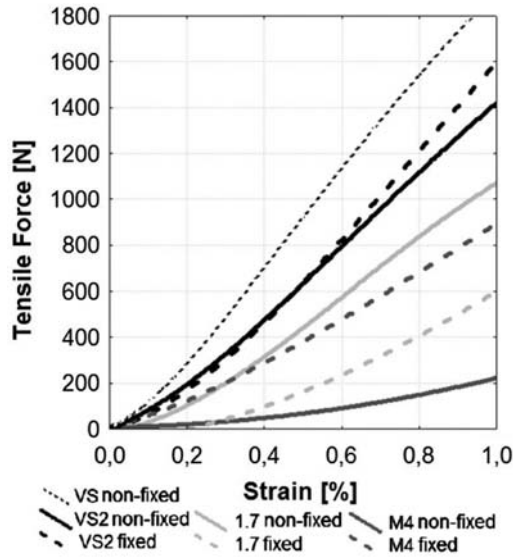


Figure 2. Tensile force – elongation curve of nonfixed and fixed samples in the 0° direction.

and consolidated hybrid yarns lead to a significantly lower tensile modulus compared with the nonfixed M1.7 samples.

A picture frame test, as described in reference [5], was conducted to record the resistance to a change in the angle of the reinforcement in relation to one another. The result of the shear force for a sample size of  $200 \times 200 \text{ mm}^2$  can be seen in Figure 3. A fabric's resistance to shear is decisive in determining the draping behavior and handling properties of a textile layer. On one hand, a fabric's tendency to be less stiff translates positively to its drapability but on the other hand, greater stiffness allows the handling of the fabric without the danger of a critical thread displacement. The properties of the biaxial knit samples are compared with a woven fabric having the same warp and weft thread count and density. The excellent

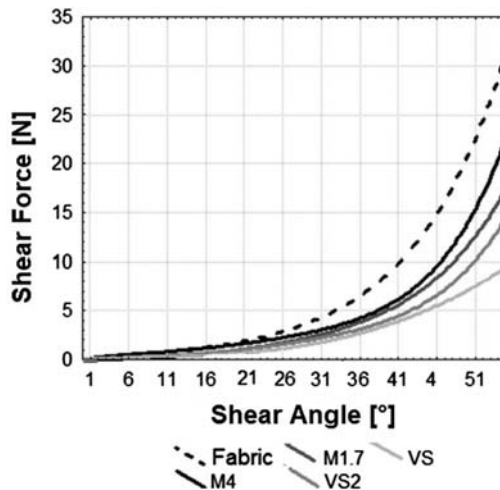


Figure 3. Shear force vs. shear angle for nonfixed samples.



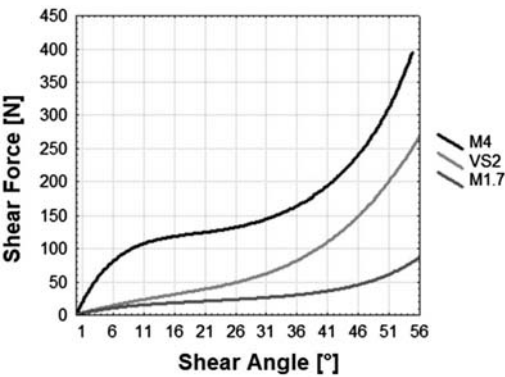


Figure 4. Shear force vs. shear angle for fixed samples.

draping behavior of the multilayer knits as compared to similar woven fabrics is clearly evident. As illustrated in Figure 3, the resistance to shear forces increases as the hybrid yarn count increases. This effect can be explained by the rough surface and the larger volume of the swirled hybrid yarns, which provides higher friction when in motion as compared to simple multifilament yarns made of glass. The graph depicts the shear angle at which the thread structure becomes so compact that a jump in the stiffness is recorded. After this angle has been reached, the shear forces typically cause wrinkles in the fabric. The critical shear angle,  $\gamma_{crit}$ , becomes smaller with an increased hybrid yarn count. The angle can be determined using the tangent method. A tangent is constructed at the beginning of the linear range. At the point where the curve deviates from the tangent line, the nonlinear stage is entered. At this point, wrinkles begin to occur in the fabric.[6]

Figure 4 depicts the results of the picture frame tests conducted on the fixed samples. A clear increase in the shear forces is seen as compared to the nonfixed samples from Figure 3. Because a stiffer fabric equates to better handling, it can be seen in this example that localized pre-consolidation of the embedded hybrid yarns offers a suitable method of structure fixation.

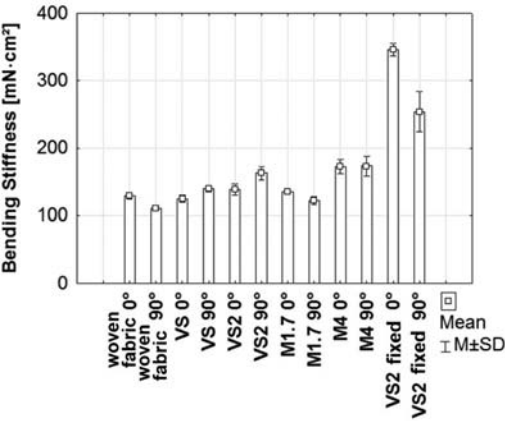


Figure 5. Bending stiffness of the nonfixed samples and the fixed sample VS2 (bars show mean values and whiskers show standard deviation).



The flexural rigidity of the fabrics was recorded using the cantilever test (as described in the DIN 53362). To determine the mechanical differences in the samples with a structural fixation, tests were conducted with both fixed and nonfixed samples. For the nonfixed samples, tests were carried out in the  $0^\circ$  and  $90^\circ$  directions because of the unsymmetrical assembly of multilayer-knitted fabrics. The fixed samples achieved such a high flexural rigidity that the test could not be carried out according to the DIN standards. Figure 5 depicts the flexural rigidity of the nonfixed samples. Since the VS2 sample, with the hybrid yarns integrated as the knitting threads, exhibited the lowest increase in flexural rigidity among the fixed samples, it could be tested using the cantilever test device. Slippage and sliding were disregarded for the tests. Preliminary testing showed that these mechanisms proved to be negligible on the samples in this study.

## 5. The derivation of a material model

### 5.1. Applied shell element

Simulating textiles pose several challenges. The microscopic construction from which the mechanical properties are derived is extremely complex and must be homogenized.[6] To achieve this, a discretization with shell elements is applicable. The thickness of the textile is much smaller than the other two in-plane dimensions. Shell elements can deal better with contact problems than beam elements. Due to the reduced number of nodes, they offer numerical advantages as compared to solid elements. In the commercial FEM program LS-DYNA, a wide selection of various shell elements is offered. For the simulations conducted in this study, fully integrated shell elements were chosen. These elements are less susceptible to numerical problems, such as hourglassing or locking effects.[7]

The size of the chosen shell elements used for the simulation depends on the warp and weft thread count (in this paper, it is 3.56 mm for every sample in the warp and weft directions). With orthogonally-constructed reinforcing layers, the position of the reinforcing threads can be determined by the position of the elements. This allows a prediction of the position of the reinforcing yarns after draping. Three integration points in the thickness direction were chosen.

### 5.2. Planar behavior

As shown in Figures 2 and 3, the tensile and shear behaviors of the textile are strongly non-linear. This can be explained by the mesoscopic construction of the textile biaxial knit. To successfully simulate a textile fabric, its nonlinear material behavior must be accounted for in the material model. Furthermore, it is necessary to introduce an appropriate deformation strain. Pure shear in textiles does not cause tensile stress in the main reinforcing direction. The orthotropic deformation properties must be considered in the model. Because the commercial FEM program LS-DYNA does not offer a suitable material model which meets all the requirements, a customized material routine was implemented for the simulations.

The Green-Lagrange deformation tensor,  $\mathbf{E}$ , describes the in-plane deformation. This tensor has previously been used to describe the deformation behavior of textiles.[8] The derivation from the deformation gradient,  $\mathbf{F}$ , is as follows:

$$\mathbf{E} = 1/2(\mathbf{F}^T \times \mathbf{F} - \mathbf{I}) \quad (1)$$

$$\mathbf{S} = \mathbf{C} : \mathbf{E} \quad (2)$$

where the material tensor is given as  $\mathbf{C}$  and  $\mathbf{S}$  denotes the second Piola–Kirchhoff Stress.

The individual membrane and bending components of the material tensor cannot be linked to one another, so as to ensure that the tensile, the flexural, and the shear rigidity observed are not coupled. Many technical textiles exhibit a high tensile rigidity with an extremely low flexural rigidity. Furthermore, the resistance to shear is independent of the tensile rigidity. An isotropic material make-up cannot properly depict the relationship of these properties. To properly depict this material behavior, an orthotropic tensor was chosen to decouple this error and reflect the mesoscopic construction.

Using the listed material tensor  $\mathbf{C}$ , the nonlinear character as well as the anisotropic structure of the textile can be described. The individual elements of the tensor used for the elastic orthotropic description are listed below:

$$\begin{aligned}
 \mathbf{C}^{1111} &= (1 - \nu_{23}\nu_{32})\mathbf{E}_1\mathbf{D}^{-1} \\
 \mathbf{C}^{2222} &= (1 - \nu_{31}\nu_{13})\mathbf{E}_2\mathbf{D}^{-1} \\
 \mathbf{C}^{3333} &= (1 - \nu_{21}\nu_{12})\mathbf{E}_3\mathbf{D}^{-1} \\
 \mathbf{C}^{1122} &= (\nu_{12} + \nu_{32}\nu_{13})\mathbf{E}_2\mathbf{D}^{-1} \\
 \mathbf{C}^{2233} &= (\nu_{23} + \nu_{21}\nu_{13})\mathbf{E}_3\mathbf{D}^{-1} \\
 \mathbf{C}^{3311} &= (\nu_{13} + \nu_{12}\nu_{23})\mathbf{E}_3\mathbf{D}^{-1} \\
 \mathbf{C}^{1212} &= \mathbf{G}_{12}\mathbf{C}^{2323} = \mathbf{G}_{23}\mathbf{C}^{3131} = \mathbf{G}_{31}
 \end{aligned} \tag{3}$$

$$\mathbf{D} = 1 - \nu_{12}\nu_{21} - \nu_{23}\nu_{32} - \nu_{31}\nu_{13} - 2\nu_{21}\nu_{13}\nu_{32}$$

As shown in Figures 2 and 3, the stiffness components are nonlinear with increasing strain, especially the components  $\mathbf{E}_1$ ,  $\mathbf{E}_2$ , and  $\mathbf{G}_{12}$ . To deal with this effect, these moduli are described by a nonlinear approach in function of the actual strain. This is exemplarily described in Equation (4) for the tensile modulus  $\mathbf{E}_1$ :

$$\mathbf{E}_1(\varepsilon_1) = \mathbf{E}_{1,0} + \mathbf{a} \cdot \varepsilon_1 + \mathbf{b} \cdot \varepsilon_1^2 + \mathbf{c} \cdot \varepsilon_1^3 + \mathbf{d} \cdot \varepsilon_1^4 + \mathbf{e} \cdot \varepsilon_1^5 \tag{4}$$

The Green-Lagrange deformation poses several advantages when examining the nonlinearity of the specific engineering constants due to the fact that it considers the current configuration of the element relative to the initial configuration. A comparison of the tested tensile and shear rigidity with the model is possible at any time step.

### 5.3. Spatial behavior

Defining the spatial behavior of nonfixed and fixed textiles poses several challenges. The flexural rigidity of textile fabrics is influenced largely by yarn-to-yarn friction inherent in the microscopic construction. The pure flexural rigidity of the reinforcing threads is negligible. Technical textiles exhibit a high Young's modulus in the reinforcing thread direction, but minimal flexural rigidity. Moreover, various and multiple levels of flexural rigidity in the fixed and nonfixed materials must be considered and factored into the definition. During fixation of the structure, the geometrical parameters remain unchanged. The tensile rigidity is minimally affected as seen in Figure 2. Despite this fact, the dimensional difference in flexural rigidity of the fixed and nonfixed samples is considerable, as depicted in Figure 5 with the VS2 specimen.

The geometrical measurements are introduced in the form of a homogenized diameter with adequate material thickness. In this respect, the Young's modulus is relatively low due to the fact that the homogenized diameter with an exact material thickness is much larger than the actual reinforcing thread diameter.

It is known, that the deflection of a beam can be divided in bending and shear deflection. [9] Because material thickness and an exact Young's modulus are nonalterable parameters, the bending stresses cannot be changed in the model. The resistance to bending deflection can be defined using the transverse shear moduli  $G_{23}$  and  $G_{31}$ , to select the flexural rigidity without the influence of the Young's modulus or diameter. Control of deflection caused by shear should be possible. Possible constraints include that the selected bending deflection is larger than the complete deflection of the fixed sample. However, it can also be the case that the bending deflection together with the maximal deflection caused from shear is not as large as the bending deflection reached by the actual textile sample.

## 6. Validation of the material model

Before the material model can be applied, a validation simulation must be conducted. The simulation approves the reproducibility of the material behavior under loading and verifies the individual deformation mechanisms that are a key in understanding the draping behavior of the textiles. Figure 6 shows the results from the strip tensile test and the picture frame test as compared to the simulation model results generated during the modeling of the testing procedures. In-plane, the material model coincides well with reality. The mechanical values for  $E_1$ ,  $E_2$ , and  $G_{12}$  could be reproduced adequately.

The flexural rigidity of the model is dependent on several parameters, including the thickness of the shell element, the existing Young's modulus, and the transverse shear module. Because the thickness of the shell and the Young's modulus are nonalterable parameters set in the initial stages of model development, the transverse shear modulus is repetitively adjusted using simulations of the cantilever rigidity test until the set flexural rigidity reflects that of the textile being tested.

Figure 7 illustrates the repetitive attempts at finding an approximation of the transverse shear modulus to the desired results. The cantilever rigidity test was reset using the characteristic measurements. The desired modulus was recorded when the sample came in contact with the  $41.5^\circ$  level. As is evident in the diagram, the calibrated material model is too rigid for an exact characterization of the biaxial knit. The influence of the transverse shear modulus is minimal. According to [10], an adequate flexural rigidity could be reached by adjusting the modulus of elasticity. To achieve this, the tensile rigidity must be greatly reduced. Table 3 compares the resulting strain with a homogenized Young's modulus of 1280 MPa and an adjusted Young's modulus to reflect a flexural rigidity of 25.7 MPa. The homogenized

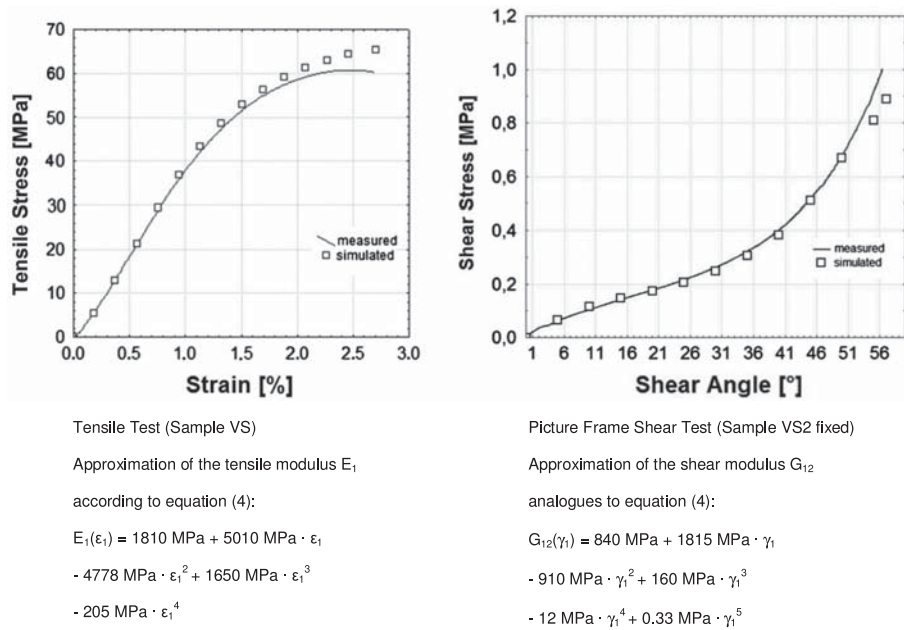


Figure 6. Comparison of the measured and simulated material values for the tensile test and the picture frame test.

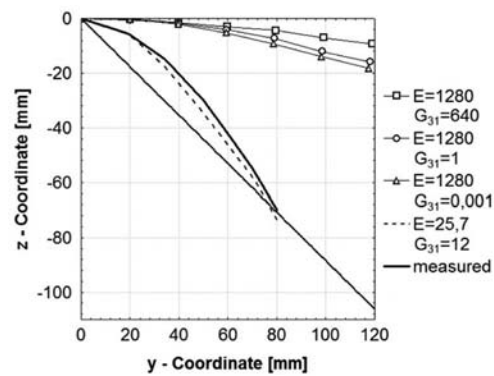


Figure 7. Repeatable approximation of the transverse shear modulus.

Table 3. Comparison of strain along the main axis after adjusting the tensile rigidity.

	$E_{\text{norm}} = 1280 \text{ MPa}$			$E_{\text{red}} = 25.7 \text{ MPa}$		
	Max.	Avrg.	Min.	Max.	Avrg.	Min.
$\epsilon_x$	$6.6 \times e^{-003}$	$5.8 \times e^{-003}$	$-3.6 \times e^{-003}$	$4.5 \times e^{-003}$	$2.5 \times e^{-003}$	$-7 \times e^{-004}$
$\epsilon_y$	$3.3 \times e^{-003}$	$4.5 \times e^{-003}$	$-5 \times e^{-003}$	$2.86 \times e^{-002}$	$2.3 \times e^{-003}$	$-9 \times e^{-004}$

Young's modulus is the fraction of the measured modulus in function of the ratio of the actual fiber cross-section to the cross-section of the used shell element as described earlier (Figure 8).

A complex-forming simulation is used for the model as seen in Figure 10. The reduced Young's modulus caused greater strain with identical loading. However, the reduced flexural rigidity leads to smaller deformation forces in the shell.

The average material strain is extremely low. Despite a greatly reduced Young's modulus, the strain remained almost the same. This can be explained by the fact that less flexural rigidity transfers less force into the system. Also, the contact forces which need to be overcome are less. The maximum strain values can be roughly compared. The strain in the pressure zones is very low and occurs only in limited areas. The peaks in strain are localized maximums occurring at the clamp mounts. To provide a conclusive comparison of the two-tension module levels, the overall displacement at the edges where the textile was pressed through the extrusion mold was examined (as seen in Figure 10). This comparison reflects the results of the individual strain areas. Table 4 lists the simulation results for the areas around the mold's edges. It is evident in Table 4 that the difference to the overall displacement at the edge areas is minimal.

To simulate the deformation behavior of the textile, shell element type 16 was chosen in the LS-DYNA and adapted with a user-defined material law. The element was able to adequately replicate the deformation behavior. However, to accurately reflect the spatial deformation behavior, the Young's modulus had to be greatly reduced. This is not satisfactory for a standard model and can lead to significant errors in complex molding simulations with high forming forces. Furthermore, the flexural rigidity cannot be accurately simulated with the

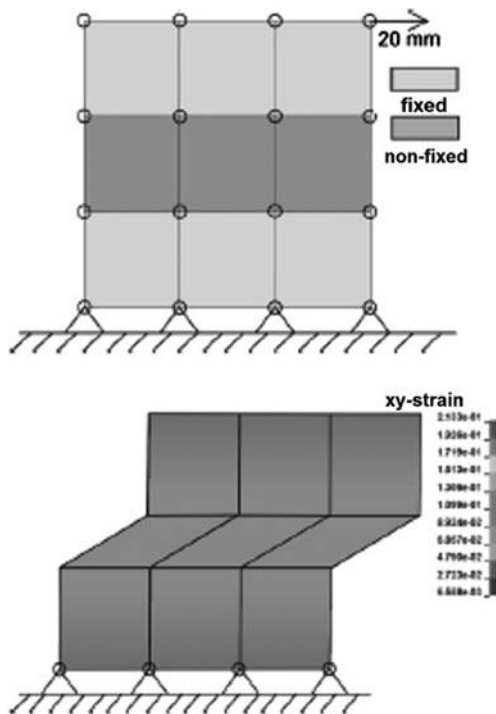


Figure 8. Simulation of occurring shear forces on a partially-fixed specimen.

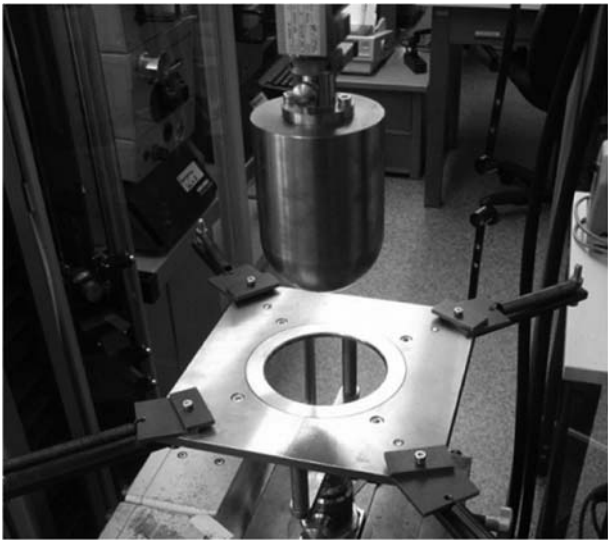


Figure 9. Hemispherical punch test stand.

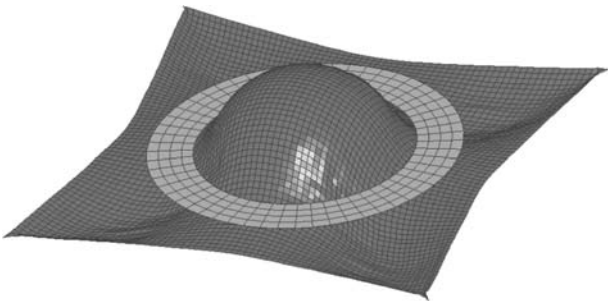


Figure 10. Simulation of the hemispherical punch test.

Table 4. Comparison of displacement at the edges.

	<i>x</i> -displacement (mm)	<i>y</i> -displacement (mm)
1280 MPa	21.32	21.46
25.7 MPa	20.72	22.02

same Young’s modulus for fixed and nonfixed textiles. Therefore, a modified formula for the material model must be found.

7. Simulation model

7.1. Varied material properties to account for fixed zones

The fixed zones present a localized change in the material properties. As is evident in the previous sections, the tensile strength is somewhat affected, whereas the shear strength and flexural rigidity are significantly changed.

To provide a simple model of these inhomogeneous properties, the existing material properties of the elements were changed in the areas where no shear occurs. This simplified method dispenses with complicated parameters and contact conditions and can be carried out in pre-processing with little effort. Adjoining elements share nodes that provide for a consistent stress state. Figure 9 exemplifies a partially-fixed shear specimen. A differentiation in the deformation rigidity of the individual zones can be clearly identified.

## 7.2. Applying the simulation model to select the zones for fixation

The first step in prefixing the textile good to improve the handling and draping properties is to locally fix areas that remain free of shear during the subsequent forming process.

This type of local fixation provides for improved handling and reduces the risk of bringing about critical thread displacements. Due to the fact that in the subsequent consolidation process of the preform to the end component a thermoset matrix system is planned, the integration of thermoplastic hybrid yarns throughout the textile should be avoided. For this reason, the thermoplastic contingent should be reduced to a minimum to avoid negatively influencing the bonding properties. Selecting fixation zones with empirical methods can be costly and time-consuming. Therefore, a simulation-aided solution is advantageous.

In the following section, the focus lies on the prefixing of the structure for the purpose of improving the handling. The fixation has no influence on the mechanical properties of the end component. Prefixing to improve the drapability is not part of this study.

After successfully validating the material model, it is possible to numerically simulate the molding process. At this point, zones can be designated where no shear occurs during the draping process. This paper describes the molding of a multilayer knit into a hemispherical shape. A test stand for this purpose is installed at the ITM at the TU Dresden. Figure 9 pictures the test stand, whereas Figure 10 illustrates the results of the hemispherical punch simulation with a nonfixed fabric. The results shown are from the biaxial knit sample VS2.

In Figure 11, it can be observed that little or no shear occurs in the main reinforcing axis from the middle of the hemisphere outwards. This area is suitable for prefixing due to the fact that a localized fixation would have no effect on the drape capability in this particular case of forming. The material feed-in system provides that the areas in the corners of the specimen remain free of shear.

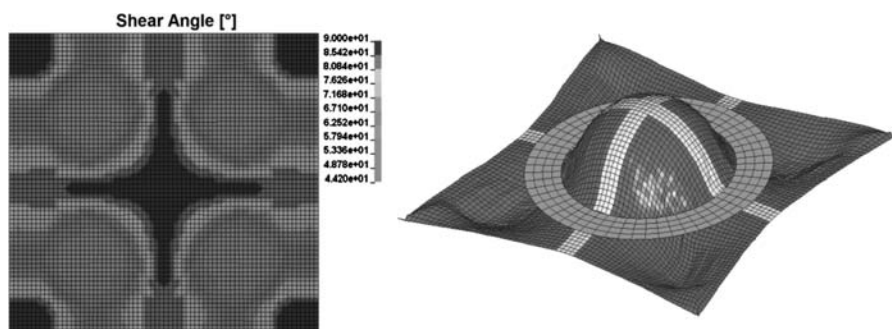


Figure 11. Shear angle after hemispherical formation (left: projection of drape results onto undeformed fabric; right: hemispherical punch simulation with fixed zones).



Should the subsequent draping process be conducted on the same molding test stand under the same conditions, then these areas could also be prefixed to improve handling.

First conclusions can be drawn from the molding simulation as to the area of the specimen which will form the end component after draping. A near-net-shaped rough pre-cut can also be derived from this simulation. The accuracy of the pre-cut depends largely on the element size. Because the element size in this simulation is oriented on the warp and weft densities, the accuracy of the pre-cut is somewhat limited. Figure 12 shows textiles as pre-cut from the simulation results. The specimen on the right is fixed in the areas as designated in the simulation from Figure 11. It is clearly evident that the fixed specimen on the right is significantly more rigid than the nonfixed specimen pictured left. The cross-like fixation creates a nearly self-stable and near-net-shaped textile preform which is extremely suitable for further processing.

Because the local fixation was only executed in those areas which could, in forefront, be designated shear-free, the fixation had no effect on the thread positioning as compared to the nonfixed pre-cut. Furthermore, the three-dimensional form can be reproduced with the same precision and without folds as the nonfixed textile preform. Figure 13 shows the fixed

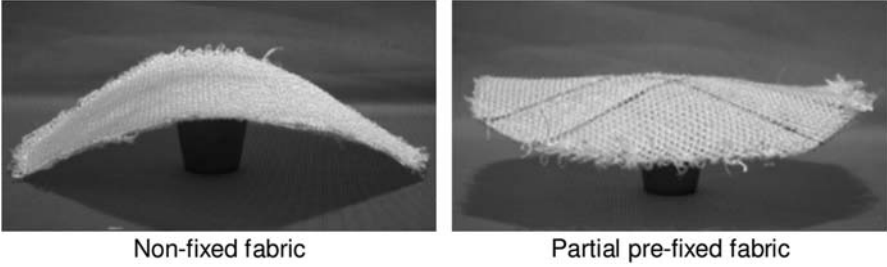


Figure 12. Rigidity of the nonfixed and fixed preform cut.

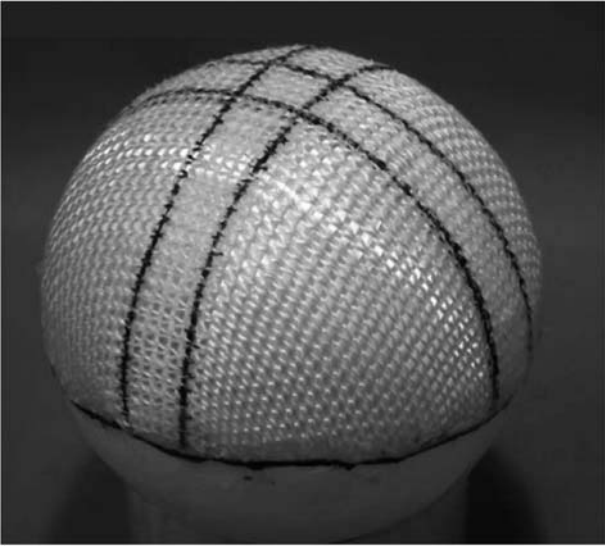


Figure 13. Formed hemisphere from multilayered knit sample VS2 with fixation zones.

preform after the draping process. The area within the lines shows the zone where the hybrid yarns were melted for fixation.

## 8. Summary and outlook

A material model could be successfully implemented into LS-DYNA to picture the significant deformation mechanisms that occur in-plane in biaxial knits. This was illustrated with simulations. A process was introduced that can be used to select zones for prefixing without influencing the draping behavior. A test demonstrator was created to explain this process in detail.

The position of the reinforcing threads after molding and the areas where wrinkles could form were successfully predicted using this method. An optical comparison excellently depicted the consistencies between the drape result and the simulation result.

Future studies should include an analysis of the influence and effects of flexural rigidity. This is indispensable to better understand and control folding and draping behavior. Furthermore, it should be a future objective to analyze and understand slippage and sliding. These mechanisms particularly offer potential in the molding and forming process and are mandatory for predicting the position of the reinforcing threads after molding.

Moreover, further studies on controlling thread position with fixation are of great interest. These studies are especially interesting since they would enable load-bearing thread positioning on the end component. Additionally, the formation of wrinkles could be avoided or shear forces could be diverted to noncritical areas of the textile.

## Acknowledgment

The authors thank the Deutsche Forschungsgemeinschaft (DFG) for the sponsorship of the DFG-AiF-Cluster 'Leichtbau und Textilien'.

## References

- [1] Abounaim Md, Diestel O, Hoffmann G, Cherif C. High performance thermoplastic composite from flat knitted multi-layer textile preform using hybrid yarn. *CST* 2011;71:511–519, ISSN 0266-3538.
- [2] Gereke T, Döbrich O, Hübner M, Cherif C. Experimental and computational composite textile reinforcement forming: a review. *Composites Part A* 2013;46:1–10, ISSN 1359-835X.
- [3] Duhovic M, Bhattachayya D. Simulating the deformation mechanism of knitted fabric composites. *Composites Part A* 2006;11:1897–1915.
- [4] Ermanni P. *Composites Technologien - Herbstsemester 2007 - Textile Halbzeuge* [Composite technologies - Autumn semester 2007 - textile materials]. Zürich: ETH Zürich, Zentrum für Strukturtechnologien; 2007.
- [5] Orawattanasrikul S. Experimentelle Analyse der Scherdeformation biaxial verstärkter Mehrlagengestricke [Experimental analysis of the shear deformation of biaxial reinforced multi-layer knits] [PhD Thesis]. Dresden: TU Dresden, Institut für Textil- und Bekleidungstechnik; 2006.
- [6] Peng X, Cao J. A dual homogenization and finite element approach for material characterization of textile composites. *Composites Part B* 2002;33:45–56, ISSN 1359-8368.
- [7] Hallquist JO. *LS-DYNA® Theory Manual*. California: Livermore Software Technology Corporation; 2006.
- [8] Cherif C. Drapierbarkeitssimulation von Verstärkungstextilien für den Einsatz in Faserverbundkunststoffen mit der Finiten-Element-Methode [Drape simulation of reinforcement textiles for the use in fiber reinforced composites with the finite element method] [PhD Thesis]. Aachen: Institut für Textiltechnik, RWTH Aachen; 1999.
- [9] Klein B. *Leichtbau - Konstruktion - Berechnungsgrundlagen und Gestaltung* [Lightweight - construction - basis of calculation and design]. Vieweg Fachbücher der Technik; 1989, ISBN 978-3-8348-0271-2.
- [10] Seif M. Bereitstellung von Materialkennwerten für die Simulation von Bekleidungsprodukten [PhD Thesis]. TU Dresden, Institut für Textil- und Bekleidungstechnik; 2007.